お茶の水女子大学自然科学報告　第50巻　第2号
Natural Science Report, Ochanomizu University, Vol. 50, No. 2 (1999)

A Morphological Approach to Volume Synthesis of Weathered Stones

Issei Fujishiro　Nao Ozawa*

Department of Information Sciences, Ochanomizu University

* Graduate School of Humanities and Sciences, Ochanomizu University

(Received November 15, 1999)

Abstract

Lack of considering aging phenomena observed frequently in the real world gives rise to unreal synthetic objects. Aging effects are viewed to play an important role in achieving seamless superposition of synthetic objects upon acquired natural scenes. Several research groups have noticed the importance of such effects, and recently reported attractive results. The primary target in this paper is weathering of stones. Stones are quite common building material; weathering also needs its specific phenomenological modeling method. Stone objects start to get eroded on their surface interacting with the open air, leading to bumpy surfaces and rounded corners. In order to simulate such effects visually, mathematical morphology (MM)-based volumetric metamorphosis is adopted. An effective morphological operator, termed weathering is devised by extending the conventional 3D opening, MM operator with stochastic structuring elements. Preliminary experiments are performed with simply-shaped stone objects to illustrate the effectiveness of the present technique.

1　Background and Purpose

Lack of considering *aging* phenomena observed commonly in the real world gives rise to unreal synthesized objects. Aging effects are viewed as playing an important role in achieving seamless superposition of synthesized objects upon acquired natural scenes, for instance, in CG montages and augmented reality environments [6]. Several research groups have noticed the importance of aging effects, and recently reported promising synthesis results [15, 12, 9, 3-5, 13, 10, 2].

Faithful computer simulation of aging phenomena based on underlying physical principles tends to be time-consuming, and impractical for *interactive* image synthesis. This is the primary reason why *phenomenological* approaches have been exploited for visual modeling of various phenomena. In addition, *controllability* is another key issue for generating a wide variety of aged objects. Most of the above-referenced existing aging methods involve their specific texture synthesis, followed by mapping the texture onto target objects, and resulting in little controllability in representing aged texture variations depending on the object shape, and the object deformation itself.

The main focus in this paper is placed on synthesis of *stone weathering*. Stones are a quite common building material; since ancient era, human beings have been utilizing stones for creating a wide spectrum of objects; e.g., buildings, bridges, belfries, and statues. They are usually exposed to wind and rain in the open for a long period, and weathered in any natural environment. Even such frequently observed phenomena need a specific phenomenological modeling method with a high degree of interactivity and controllability.

Stone objects, which are generally composed of different kinds of minerals intermixed with one another, start eroding on their surfaces interacting with the open air, leading to bumpy surfaces and rounded corners. Sometimes, fragile portions with high curvature are completely removed. It is obvious that such complex deformations cannot be achieved with traditional free-form deformation nor rounding operation on solid

models. Volumetric morphing and warping have already appeared in the literature [8, 20]. However, the techniques cannot be applied directly to the simulation of weathering. The primary reasons are two-fold:

- Plausible target volume locally with high frequency components and globally with simpler topology cannot be given a priori for a given source volume.
- Weathering operation is intrinsically stochastic, reflecting the physical and chemical randomness of mineral fabric with the effect of wind and rain.

Perlin and Hoffert [15, 16] present the *hypertexture* and *surflet* approaches which generate an eroded cube by taking the intersection of a cube and a fractal sphere. However, the approaches are not guaranteed to generate the same erosion effect for a given arbitrarily-shaped object. In other words, it is unclear how to determine the number, location and size of fractal spheres depending on the target object geometry. An attractive texture synthesis method related to these approaches is reported by Dischler, et al. [2], where a mineral-like, macro-structured texture is synthesized by using their image- and skeleton-based approach.

Dorsey, et al. [5] propose a volumetric model of near-boundary, multi-layered structure of stones, and simulate the stone weathering process by solving a specific system of finite difference equations governing the moisture-mineral interaction. As for the realistic rendering of weathered stones, they successfully take advantage of their earlier technique called *subsurface scattering*, as in [3].

This paper attempts to simulate the effects of stone weathering in a more abstract manner than the Dorsey method by *mathematical morphology* (MM)-based volumetric metamorphosis. MM, which was originally proposed by Matheron [7], provides a quite simple algebraic structure of morphological operations, which are constructed basically by *dilation* and *erosion*, plus a few other auxiliary operators. Dilation and erosion have the effect of "expanding" and "shrinking" of a region, respectively. The algebraic structure of MM allows for straightforward building block-oriented implementation of complex morphological operations. Adjustment of an argument, called *structuring element* (SE), to the operators can lead to the ease of generating various deformation effects. MM is expected to serve as a good abstraction of stone weathering, because it is well known that practical weathering is developed by iterated dilations and erosions of stones due to water-crack interactions. Indeed, an effective MM operator, termed *weathering*, is devised herein by extending the ordinal 3D *opening* MM operator with stochastic structuring elements.

The remainder of this paper is organized as follows. The next section clarifies the reason why the opening operator is chosen as the basis for designing the weathering operator. Section 3 is devoted to the detailed description of the weathering operator in the digital setting. In Section.4, several preliminary experiments are performed with simple-shaped stone objects to illustrate the effectiveness of the present technique. More sophisticated examples are also visualized. Section 5 summarizes the paper with some remarks on the future research directions.

2 Basic Idea

Conventionally, MM has been used as a unified framework for image (2D) and signal (1D) analysis [7]. An extension of MM to volume (3D) has also been reported (e.g., [17]), where the main goal is limited to volume analysis, including noise elimination. On the contrary, this paper strives to adopt the 3D digital MM for the purpose of volume synthesis.

2.1 2D Opening

First, our primary attention is paid to an MM operator, called *opening*. For brevity, the effect of Euclidean opening is illustrated herein with a 2D example.

The definition of opening is as follows:

$$opening(A,E) = dilation[erosion(A,E)] \quad A\text{: binary image, } E\text{: SE}$$

As for more specific definitions of dilation and erosion in 3D, see Subsection 3.1.

An execution example of 2D opening is shown in Fig.1. It is observed clearly from Fig.1 that the following three dominant deformation effects due to opening are akin to those due to actual weathering:

(1) Corners are rounded;

(2) Protruded portions are eroded; and

(3) Small portions with high curvature are possibly removed.

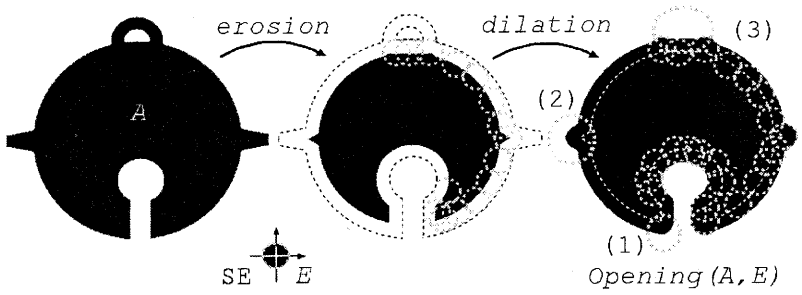

Figure 1. 2D opening: an example.

It should be noted here that all these effects cannot be achieved only with the erosion operator. This is the main reason why opening is adopted as the basis for devising the weathering operator. In addition, the degree of the above-described features can be controlled by the selection of shape and size of SE. Especially, a dynamic circular SE with perturbed radius is expected to produce a stochastic nature of real weathered stones more effectively. This is the heart of the extension of opening to weathering in the next section.

3 Weathering Operator

The 3D digital binary MM is employed herein to establish a practical environment for morphological deformation of volumes.

3.1 3D Opening

Volumetric objects are represented with a set of binary voxels whose values are 1. Let A and B denote two objects. $A \subset B$ *iff* any "1"voxel in A is also an element of B. Fig.2 shows a tiny volumetric object data and its set representation.

Next, the definition of 3D dilation and erosion in the digital setting are provided. Herein, *trans* denotes the *translation* operator, which is defined as follows:

$$trans(A;i,j,k) = \{(l_t,m_t,n_t) \mid l_t = l+i, m_t = m+j, n_t = n+k, (l,m,n) \in A\}$$

The dilation operator is defined as the union of each of A's voxels which is translated with an element in E:

$$dilation(A,E) = \mathrm{Y}_{(i_n,j_n,k_n)\in E} trans(A;i_n,j_n,k_n)$$

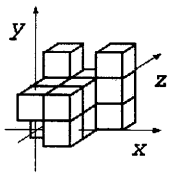

A = {(1,0,0), (0,1,0), (1,1,0),
(0,0,1),..., (1,1,2),
(2,1,2),(0,2,2),(2,2,2)}

Figure 2. Set representation of volume.

On the other hand, the erosion operator is defined as the intersection of each of A's voxels which is translated with an element in E in the negative direction:

$$erosion(A,E) = \mathrm{I}_{(i_n,j_n,k_n)\in E} trans(A;-i_n,-j_n,-k_n)$$

As in 2D, 3D opening operator is defined with dilation and erosion, as follows:

$$opening(A,E) = dilation[erosion(A,E),E]$$

Fig.3 depicts the block diagram of opening.

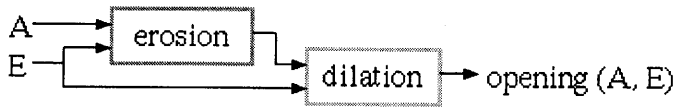

Figure 3. Block diagram of opening

Fig.4 illustrates an opening process for A given in Fig.2 with an SE E = {(0,0,0), (1,0,0)}.

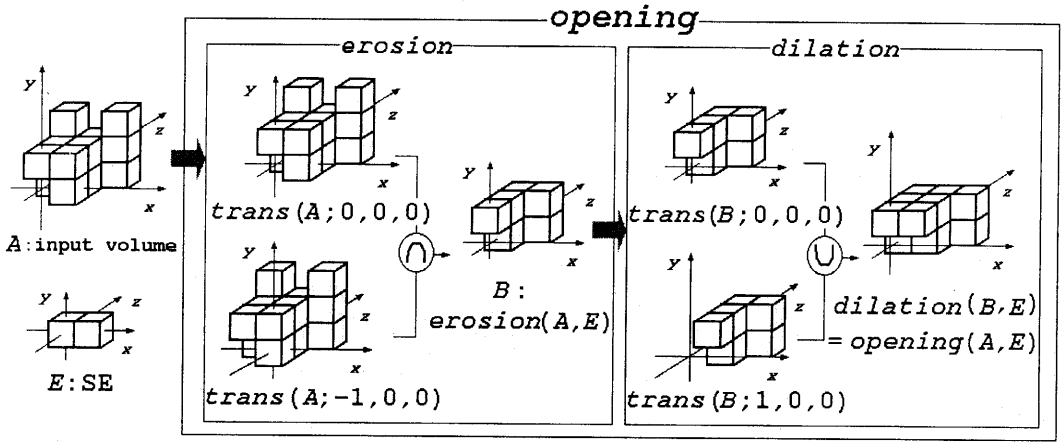

Figure 4. 3D opening: An example.

3.2 Weathering Operator

As described in the previous section, the deformation effect of the opening operator is deterministic. In order to account for the stochastic nature of real weathering phenomena, the *weathering* operator uses $erosion_p$, which differs from the original erosion in that the SE size changes, reflecting the kind of mineral corresponding to the voxel located at the center of the SE. Specifically, another *material* volume M is introduced, whose size is the same as that of the original *shape* volume A, and when each voxel in the material volume M is referred to, predefined transfer functions are evaluated to map the kind of material to its corresponding SE size. The more fragile the mineral of a voxel is, the bigger the averaged radius is given to the spherical SE centered at the voxel. An example of *SE transfer functions* $W(m)$ and $s(m)$ is plotted in Fig.5, where each of the three kinds of minerals is identified with its interval of voxel field m, and is given its stochastic SE with radius $W(m)$ and perturbation width $s(m)$. The actual SE radius is given within the interval $[w(m)\text{-}s\ (m),\ w(m)+s\ (m)]$. Consequently, $erosion_p$ is defined as follows:

$$erosion_p(A,E) = \mathrm{I}_{(i_n,j_n,k_n)\in E} trans(A;(W(m)+\varepsilon)\cdot(-i_n,-j_n,-k_n)) \qquad (|\ \varepsilon\ | \leq s(m)) \qquad (1)$$

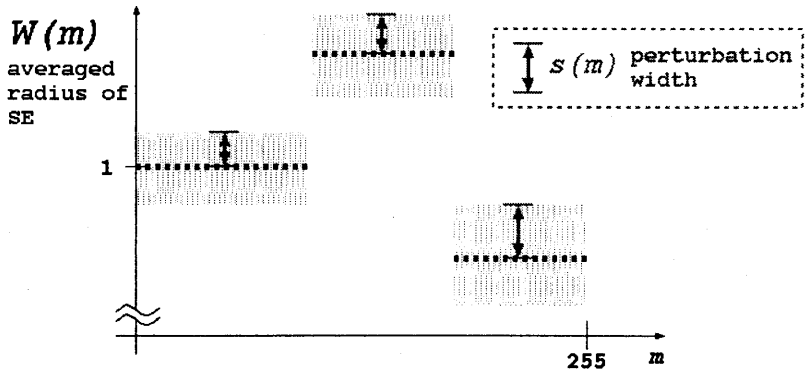

Figure 5. Example of SE transfer functions definition.

Fig.6 shows the block diagram of weathering. Note that the $erosion_p$-*dilation* path is intersected with the opened A, so as not to dilate the resulting shape relative to A.

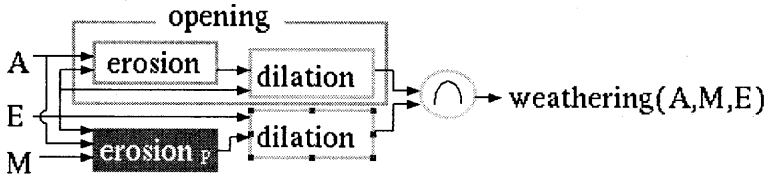

Figure 6. Block diagram of weathering.

4. Preliminary Experiments

The present MM-based volume modeling and manipulation environment was implemented, and the following experiments were performed on an SGI O2 system (CPU: R10000, Clock: 195MHz, RAM: 256MB). To simulate volumetric global illumination, a volumetric ray-tracer [18] incorporated in the VolVis2.1 system

(http://www.cs.sunysb.edu/~vislab/volvis_home.html) was employed. *VolVis* [1] is a comprehensive, diversified, and high performance volume visualizer that has been developed at the State University of New York at Stony Brook, and is available as freeware. The visualizer makes it possible to evaluate the visual effects of the above-described operators justifiably with standard volumetric simulation of light absorption, reflection, and refraction on stone surfaces.

In the modeling of bell-shaped test volumes, the binary shape volume was created by CSG operations, and then voxelized into a 230x230x230 volume data set (Fig.7(a)). Of course, *volumetric sculpting* [21] could be used as an alternative way to model stony objects effectively in a volumetric fashion. On the other hand, the material volume was obtained simply by piling up a series of stone cross-sectional images whose pixels are randomly permuted (Fig.7(b)). The size of the material volume is the same as that of the shape volume. Then, solid texturing [14] was performed with the shape volume and the material volume. A ray-traced image of the resulting stone volume is shown in Fig.7(c). The averaged rendering time was approximately 7 minutes.

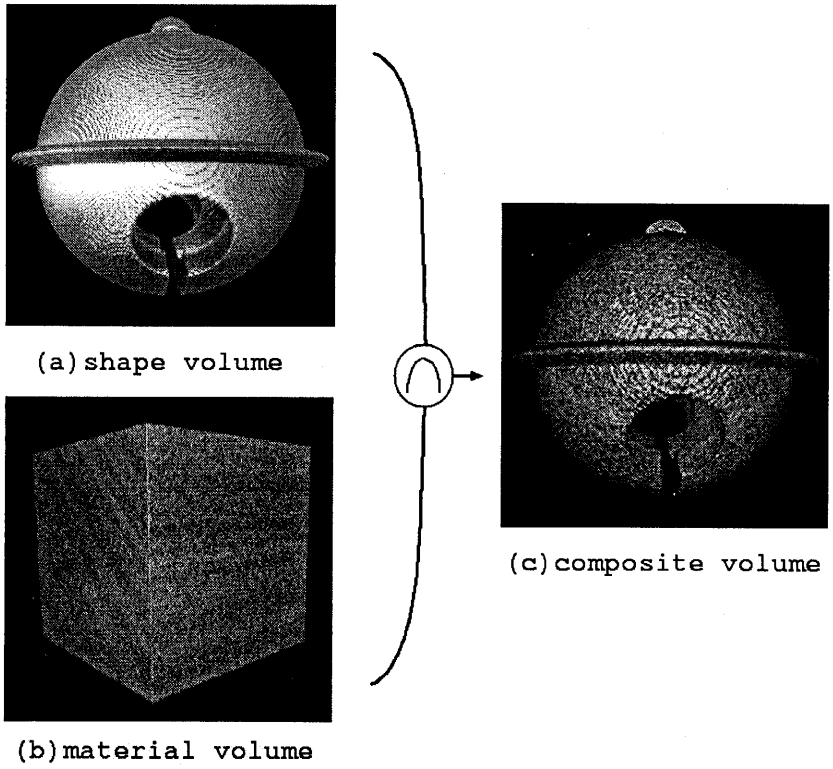

Figure 7. Solid texturing for producing bell-shaped test volume.

4.1 Opening v.s. Weathering

Fig.8(a) is the resulting image which illustrates how the application of an opening operator transforms the bell-shaped object. It took 90 minutes to execute the opening operator, whose SE has a 6 voxel radius, on the original shape volume. The rendering time was 6 minutes, almost the same as in the case of the original volume in Fig.7(c). This implies the well-known intrinsic advantage of volume graphics, that is, the temporal complexity is nearly independent of volumetric contents. Comparing Fig.8(a) to Fig.7(c) reveals not only that all the corners are rounded, but also that there remains only the protruded decorative horizontal band, while the top small handle is completely removed.

Fig.8(b) is the resulting image of the bell-shaped object to which the weathering operator was applied. The common material volume contains three different minerals, each of which is assigned its own interval value

for the radius of SE. The averaged size of the used SE is the same as in the opening, but the radius of the SE has a 2 voxel-wide perturbation. The rendering time was 8 minutes. It is observed from Fig.8(b) that the weathering operator generates the weathered stone bell-shaped object more naturally with a bumpy surface including even a few pits, and a partially eroded band.

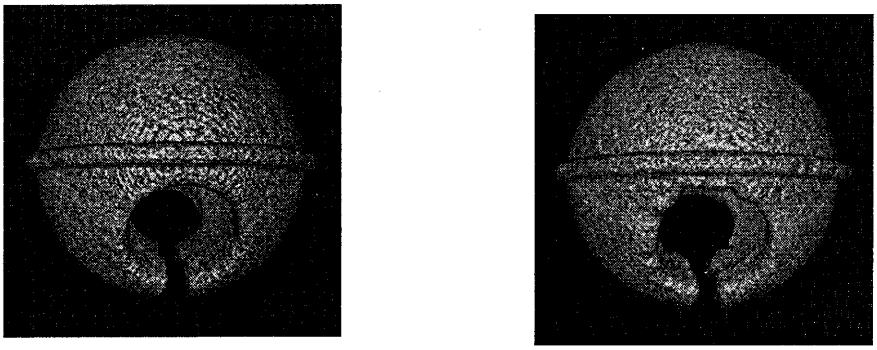

(a) After opening (b) After weathering

Figure 8. Experimental result: Bell-shaped object.

4.2 Iterative Application of Weathering

The conventional opening satisfies the idempotence property [7]:

$$opening[opening(A,E),E] = opening(A,E)$$

From the viewpoint of volumetric metamorphosis, it implies that once a given volume is opened, the resulting volume gives a limit of transformability. Such a property does not hold for weathering, because the employed $erosion_p$ has a stochastic nature (see Eq. 1). In general, the following relationship holds:

$$weathering(A,E) \subset opening(A,E)$$

As described in Section 1, practical weathering is developed by iterated dilations and erosions of stones due to water-crack interactions. The goal of the second experiment is to observe what effects are produced by iterated application of a weathering operator with a smaller SE. Fig.9 depicts the block diagram for the experiment.

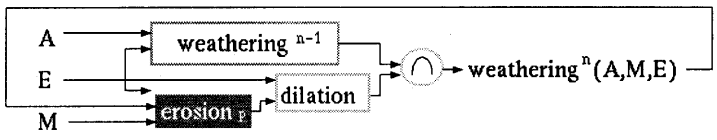

Figure 9. Block diagram of iterative weathering.

The same bell-shaped object volume of the previous section is used herein. Fig.10 shows a sequence of images where the original volume is weathered iteratively (up to 5 times) with an SE whose radius is 4. It can be observed from the sequence that iterative application of weathering can control the length of period the target object is exposed to the open air.

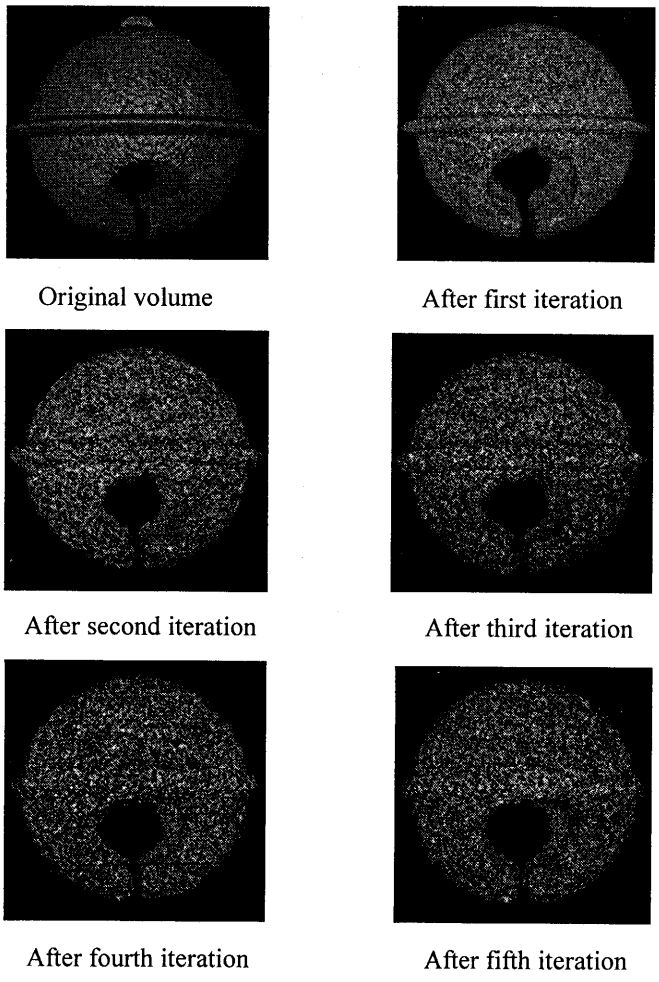

Figure 10. The result of iterative weathering.

4.3 More Sophisticated Examples

Fig.11 shows a natural scene image of a virtual thicket, on which an *ancient doll* synthesized with the present method is superposed. The size of the doll volume is 168x240x168. Note that a slight vestige of face featuresremains, which is hard to be created with currently-available shape modelers. *Volumetric accessibility*

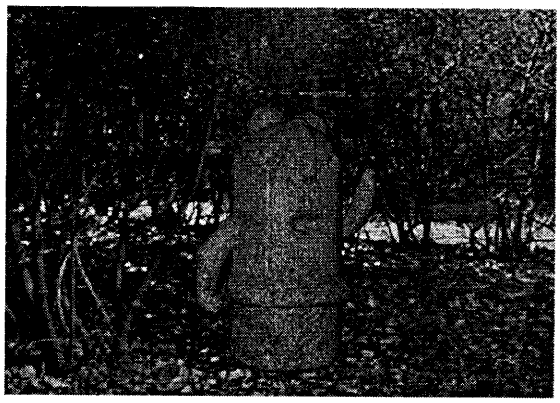

Figure 11. Ancient doll.

proposed in [12] could be also computed to identify the hollow area and map a moss-covered texture on it.

Fig.12 shows another piece inspired by a European old castle whose wall is made of bricks jointed with cement mortar. The size of the entire volume is 255x230x230. In this case, a single brick is modeled with a subvolume whose size is 8x8x6. Different SE sizes are given to bricks and cement mortar. It is observed that the top of the wall and the window frames are weather-beaten.

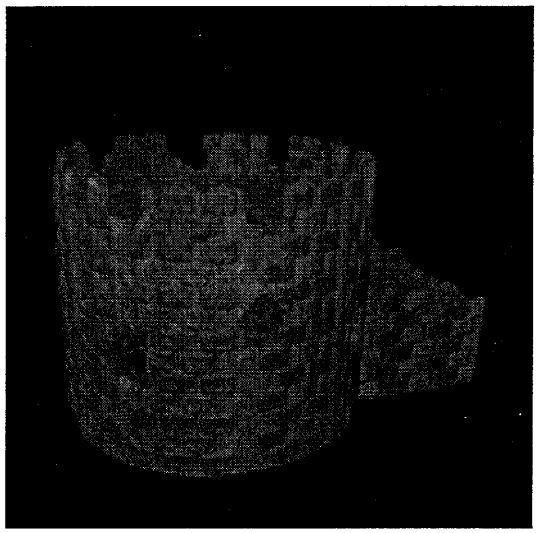

Figure 12. An old castle.

5. Concluding Notes

This paper has presented a 3D morphological approach to visual simulation of weathering effects on stone objects. Preliminary experiments proved that the present morphological operator can produce visual effects similar to actual weathering. There still remain several research issues. In order to provide an interactive environment for the handling of volumes, the improvement of temporal complexity of weathering operator is crucial. The time to calculate $erosion_p$ in Eq. 1 is strongly influenced by the cardinality of SE. One candidate for accelerating the computation is to evaluate $erosion_p$ only with boundary voxels in SE. In addition, iterative calculation of $W(m)+\varepsilon$ by calling a random number generator is another time-consuming part in Eq. 1. Accelerated calculation can be achieved by hash function-based access to a pre-calculated random number table [11].

The material volume used in this paper is insufficient to represent the actual fabric of stones. Solid texture generation based on primitive instancing and incomplete tessellation of minerals [19] is an attractive way to generate more realistic stone material. The present weathering operator should be enhanced by using gray-scale MM [7] for making SE transfer functions more precise by reflecting the local properties of mineral fabric structure of stones.

Further extensions to the weathering operator should account for:

- Strength and vulnerability of minerals;
- Anisotropy due to global thermodynamical structure of stratums, such as joints;
- Flow of rain and wind on the surface of stone objects.

Addition of crack effects due to other factors such as botanical root growth is another challenging theme for synthesizing more realistic stone-related aging phenomena.

Acknowledgements

The authors gratefully acknowledge Xiaoyang Mao, Mikio Iizuka, and Karen Vierow for their helpful comments and suggestions. Etsuko Aoki helped the authors in preparing the final draft of this paper.

References

1. Avila R, He T, Hong L, Kaufman A, Pfister H, Silva C, Sobierajski L, Wang S. VolVis: A diversified volume visualization system. In: *Proc. Visualization '94*; 31-38.
2. Dischler J-M, Ghazanfarpour D. Interactive image-based modeling of macrostructured textures. *CG&A* 1999; **19**(1):66-74.
3. Dorsey J, Hanrahan P. Modeling and rendering of metallic patinas. In: *Proc. SIGGRAPH96*; 387-396.
4. Dorsey J, Pedersen HK, Hanrahan P. Flow and changes in appearance. In: *Proc. SIGGRAPH 96*; 411-420.
5. Dorsey J, Edelman A, Jensen HW, Legakis J, Pedersen HK. Modeling and rendering of weathered stones. In: *Proc. SIGGRAPH 99*; 225-234.
6. Fujishiro I, Ozawa N. Synthesizing weathered objects for seamless super-imposition on natural scenes (abstract). In: *Conference Abstracts of ISMR'99*.
7. Giardina CR, Dougherty ER. *Morphological Methods in Image and Signal Processing*. Prentice Hall, Engelwoods Cliffs, 1987.
8. He T, Wang S, Kaufman A. Wavelet-based volume morphing. In: *Proc. Visualization '94*; 85-91.
9. Hsu S, Wong T. Simulating dust accumulation. *CG&A*, 1995; **15**(1):18-22.
10. Hirota K, Tanoue Y, Kaneko T. Generation of crack patterns with a physical model. *The Visual Computer* 1998; **14**(3):126-137.
11. Mao X, Kikukawa M, Fujita N, Imamiya A. Line integral convolution for 3D surfaces. In: Lefer W, Grave M (eds) *Visualization in Scientific Computing '97*. Springer-Verlag, Wien New York, 1997; 57-69.
12. Miller G. Efficient algorithm for local and global accessibility shading. In: *Proc. SIGGRAPH 94*; 319-326.
13. Ozawa N, Fujishiro I. Rendering of metallic patinas with cleaning effect (in Japanese). In: *IPSJ SIG notes*, 97-CG-87 October 1997; 13-18.
14. Perlin K. An image synthesizer. In: *Proc. SIGGRAPH'85*; 287-296.
15. Perlin,K, Hoffert EM. Hypertexture. In: *Proc. SIGGRAPH '89*; 253-262.
16. Perlin K. Surflets. In: Inakage M (organized) *Photorealistic Volume Modeling and Rendering Techniques. SIGGRAPH '91 Course Notes* 27; 4-1-21.
17. Sakas G, Walter S. Extracting surfaces from fuzzy 3D-ultrasound data. In: *Proc. SIGGRAPH 95*; 465-474.
18. Sobierajski LM, Kaufman AE. Volumetric ray tracing. In: *Proc. 1994 Symposium on Volume Visualization*; 11-18.
19. Takagi S, Fujishiro I. Microscopic structural modeling of colored pencil drawings (abstract). In: *Visual Proc. SIGGRAPH 97*; 187.
20. True TJ, Hughes JF. Volume warping. In: *Proc. Visualization '92*; 308-315.
21. Wang SW, Kaufman AE. Volume sculpting. In: *Proc. 1995 Symposium on Interactive 3D Graphics*; 151-156.